

Seismic Intensity Measures for Probabilistic Demand Modeling of Rocking Rigid Components

Jieun Hur

Visiting Assistant Professor, Civil, Environmental and Geodetic Engineering, The Ohio State University, Columbus, Ohio, U.S.A.

Abdollah Shafieezadeh

Assistant Professor, Civil, Environmental and Geodetic Engineering, The Ohio State University, Columbus, Ohio, U.S.A.

ABSTRACT: Nonstructural components such as electrical equipment have critical roles in the proper functionality of various infrastructure systems. Some of these devices in certain facilities should operate even under strong seismic shakings. However, it is challenging to define each mechanical and operational failure and determine system failure probabilities under seismic shakings due to the uncertainties in earthquake excitations and the diversity of electrical equipment, among other factors. Therefore, it is necessary to develop effective and practical probabilistic models for performance assessment of electrical equipment considering variations in equipment features and earthquakes. This study will enhance the understanding of the rocking behavior of nonstructural equipment and linear to nonlinear behavior of restrainers. In addition, the present study will generate probabilistic seismic demand models of rigid equipment for a set of conventional and novel intensity measures.

1. INTRODUCTION

Previous research studies developed numerical models of nonstructural components to capture their dynamic behavior. A number of studies also performed shake table tests on these equipment. Results of these investigations showed that the dynamic characteristics of nonstructural components are very sensitive to the support boundary conditions. This is expected since components such as electrical equipment are relatively rigid structures. Furthermore, investigation of damage to nonstructural components during recent earthquakes revealed that the base restrainers of electrical and mechanical equipment sustained damage and therefore, allowing the equipment to rock and slide with high response accelerations. Even though standards such as IEEE/ANSI and FEMA highly recommend that all essential equipment be fully restrained in seismic zones, in many cases, heavy nonstructural components such as electrical and mechanical equipment are installed without

complete base restraints, leading to sliding and rocking behavior under seismic shakings.

In order to estimate the seismic performance of general types of electrical cabinets, this study will consider various physical features of such devices and generates representative samples using Latin Hypercube Sampling (LHS). The seismic behavior will be analyzed considering the nonlinear behavior of restrainers as well as the rocking behavior of rigid components, which is critical for relatively slender electrical cabinets. In addition, various characteristics of earthquakes will be considered in this study using a large set of ground motion records. The results will be presented in the form of probabilistic seismic demand models (PSDMs). Finally, this study explores the performance of commonly used intensity measures for probabilistic seismic demand modeling of rigid components and proposes a new intensity measure to achieve more reliable PSDMs.

2. DYNAMIC BEHAVIOR OF RIGID BLOCOS WITH NONLINEAR RESTRAINERS

2.1. Previous Works

The seismic performance of electrical cabinets highly depends on their rocking behavior which is controlled by the performance of restrainers. Shenton et al. (1996) and Taniguchi (2002) classified the nonlinear behavior of unrestrained rigid blocks subjected to horizontal and vertical base excitations. Yim et al. (1980) derived the governing equations of motion for the rocking behavior of unanchored blocks subjected to seismic shakings and presented their response sensitivity to the properties of ground motions. Makris and Zhang (2001) developed analytical models for the rocking behavior of anchored (restrained) blocks under horizontal pulse-type as well as earthquake ground motions. Using the analytical models, Makris and Zhang (2002) investigated the magnitude of the horizontal pulse required for overturning the block. However, their analytical models assume that the blocks perfectly rock without re-bouncing back into the same falling back direction. Therefore, the analytical rocking models had fictitious values of the coefficient of restitution based on the slenderness ratio of blocks. Gupta et al. (1999) and Yang et al. (2003) suggested Ritz vector approach to estimate the rocking behavior of restrained electrical cabinets. Hur (2012) described previous problems of analytical models of restrained components, and Hur and Shafieezadeh (2013) suggested a new analytical model for restrained components with rocking behavior. Their model considered the nonlinear behavior of two independent restrainers for the rocking behavior of a rigid block using a Bouc-Wen model.

2.2. Analytical Model of Rocking Blocks

Figure 1(a) shows a restrained rigid block with height ($H = 2h$), and width ($B = 2b$). The mass m is located at the center, and R is the distance from the bottom edge to the center. As the restrainer deforms, this block starts rotating with angular displacement, θ , under horizontal excitations.

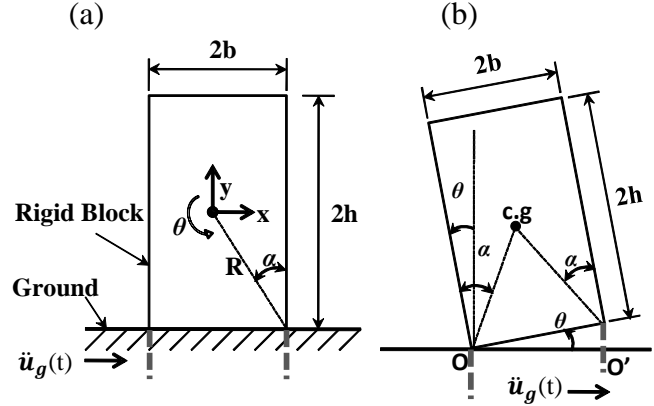


Figure 1. Schematic restrained block of rocking motion

As shown in Figure 1, the rotating behavior of the block depends on its geometry and restraint type. Based on the equations of Makris and Zhang (2001), Hur and Shafieezadeh (2013) developed models for rocking behavior of restrained rigid blocks as shown in Equations (1-2).

The angular mass moment of inertia, I_o , about the center of rotation is $4/3 * W/g * R^2$ considering that the total mass is $m = W/g$, where W is the weight of the block and g is the acceleration due to gravity. It is assumed that the mass is uniformly distributed over the area of the rectangular block. The block oscillates about the centers of rotation O and O' as shown in Fig. 1 (b).

$$I_o \ddot{\theta}(t) + mgR \sin[\alpha - \theta(t)] + 4Kb^2 \theta_y Z(t) \cos \frac{\theta(t)}{2} = -m \ddot{u}_g(t) R \cos[\alpha - \theta(t)], \quad \theta(t) > 0 \quad (1)$$

$$I_o \ddot{\theta}(t) + mgR \sin[-\alpha - \theta(t)] + 4Kb^2 \theta_y Z(t) \cos \frac{\theta(t)}{2} = -m \ddot{u}_g(t) R \cos[-\alpha - \theta(t)], \quad \theta(t) > 0 \quad (2)$$

In these formulations, \ddot{u}_g is the horizontal excitation, K is the stiffness of restrainers, and θ_y is the rotational angle at which the restrainers yield. $Z(t)$ is the hysteretic dimensionless quantity determined as part of the Bouc-Wen model. The angle $\alpha = \tan^{-1}(b/h)$ is a measure of the slenderness of the block. α and θ_y define the tipping point of the block. It is assumed that the

value of $\theta_y \ll \alpha$. Therefore, when the rotational angle response (θ) of the block passes θ_y , the restrainer starts yielding. When θ reaches the critical angle α , the block approaches the bifurcation of stable and unstable states. That is, when $|\theta| > \alpha$, the block falls over due to the overturning moment of the gravity load and then cannot return to the original position without an additional restoring force. However, the block experiences a rocking or oscillatory motion when $|\theta| < \alpha$.

3. SEISMIC PERFORMANCE OF RIGID BLOCOS WITH NONLINEAR RESTRAINERS

3.1. Generating Samples of Electrical Cabinets

3.1.1. Physical Features of Electrical Cabinets

Electrical cabinets enclose various components such as switches, circuit breakers, displays, and conductors (buses). There are several manufactures in the U.S. that produce different types, size, and modules of cabinets according to the National Electrical Manufacturers Association (NEMA) standards. This study will focus on the physical features of low-voltage switchboards from three major manufacturers in the U.S. The height of all modules from three manufacturers ranges from 90 to 92 inches. The width varies between 22 inches and 48 inches. The depth of enclosures depends on the usage and demand of customers, and therefore the weight of the unit is diverse depending on the width and the quantity of components mounted in the cabinet. Considering the specifications of electrical cabinets, multiple parameters are considered to characterize the physical features, and each parameter has a different distribution. Since these parameters and their distributions result in diverse combinations of features, it is important to generate appropriate and effective collections of parameters for simulation purposes. In this study, Latin hypercube sampling (LHS) is used, which is a statistical method for the random generation of a collection of parameter values from probability

distributions. A total of 720 sample sets are generated in this study.

Table 1 shows the set of geometrical and physical parameters of electrical cabinets considered in this research. It contains various parameters to represent enclosures and additional devices, switches, and conductors inside. In order to observe the critical rocking behavior of cabinets, relatively slender electrical cabinets which have narrow depths are selected.

Table 1. Geometrical and Physical Parameters of Electrical Cabinets (UNIT: inch/mm, lbf/kgf)

Parameter	Distribution	
Height (H)	Constant: 91.5/2324	
Width (B)	Discrete: 24-54/610-1370	Uniform distribution
Depth (D)	Discrete: 16-32/400-810	Uniform distribution
Total Weight (W_{total})	Discrete +Continues: 500-1340/225-610	Normal distribution

General enclosures of electrical cabinets are made of steel plates according to ANSI code for the quality of electrical equipment. They are standardized with specific modules from each manufacturer. Based on the product information from S-company, this study assumed the height, depth, and width of cabinets shown in Table 1. It is important to estimate the total weight considering various parameters, since the total weight of cabinets is converted to their mass which affect their dynamic behavior under seismic shakings. The weight of cabinets significantly varies and depends on the size of enclosures and the number and types of components mounted in the cabinets. The total weight of one unit can be determined as the sum of the weight of the enclosure ($W_{enclosure}$), components (W_{comp}), and miscellaneous items (W_{mis}) as shown in Eq.(3). $W_{enclosure}$ can be estimated using the unit weight (w_s) per surface area of the enclosure and the surface of the enclosure including four vertical faces and

top/ceiling cover as given in Eq.(4). The average unit weight (w_s) for the enclosure is assumed as 0.042 psi (0.00003 kgf/mm²) with a normal distribution. W_{comp} is computed considering the type and quantity of buses/conductors, circuit breakers, switches, and auxiliary components in the unit. In addition, the weight and quantity of buses/conductors depend on the ampacity of the equipment. Therefore, the depth of unit and ampacity are randomly selected considering their dependency, and W_{comp} is estimated as given in Eq.(5), where w_i is the weight of a component, and n_i is the quantity of that component in the cabinet.

$$W_{total} = W_{enclosure} + W_{comp} + W_{mis} \quad (3)$$

$$W_{enclosure} = w_s \times \text{surface of enclosure} \quad (4)$$

$$W_{components} = \sum_i w_i \times n_i \quad (5)$$

3.1.2. Rocking stiffness of restrained electrical cabinets

In order to evaluate the dynamic behavior of restrained cabinets, simplified but representative rocking stiffness models are needed. This study referred to the work of Yang et al. (2003) and Gupta et al. (1999) that formulated a rocking stiffness of restrained electrical cabinets using the Ritz vector approach. They derived the equations for rotational stiffness (K_θ) through a parameter study. This value depends on the number of bolt connections (N), bolt distance (Δ_b), thickness of steel plate (t), and the length of moment arms ($D - \Delta_b$) which is the distance from the bolt to the rotational axis. According to the configuration of electrical cabinets, the rotational stiffness (K_θ) is determined as given in Eqs. (6-7).

$$K_\theta = 13.30(\sum_{i=1}^N c_i^2)D^2 \frac{Et^3}{12(1-\nu^2)} \frac{1}{\Delta_b^2} \quad (6)$$

for $0.1 \text{ in} \leq t \leq 0.2 \text{ in}$; $1.0 \text{ in} \leq \Delta_b \leq 2.0 \text{ in}$; $16 \text{ in} \leq D \leq 24 \text{ in}$, and

$$K_\theta = 16.44 \frac{Et^3}{12(1-\nu^2)} \frac{1}{\Delta_b^2} \quad (7)$$

for $0.2 \text{ in} \leq t \leq 0.4 \text{ in}$; $2.25 \text{ in} \leq \Delta_b \leq 3.25 \text{ in}$; $25 \text{ in} \leq D \leq 36 \text{ in}$

In above equations, C is assumed as a constant value of 16.44. Based on these equations and collected data from 3.1.1, K_θ is computed with a normal distribution. Using this K_θ , the vertical stiffness of each restrainer, K , is computed for Eqs.(1-2).

3.2. Selection of Ground Motion Records

The ground motion records for this study are chosen from a set of records generated by Baker et al. (2011). These ground motions have been used in a variety of applications, including analysis of structural and geotechnical systems at various locations throughout California (or other active areas where seismic hazard is dominated by mid- to large-magnitude crustal earthquakes at near to moderate distances). The standardized sets of ground motions include a wide range of periods and near-fault directivity pulses as well. They were matched to the uniform hazard spectrum and associated causal events for a site in Oakland, California. These motions were selected to represent the ground motion hazard at each of three 2%, 10%, and 50% in 50 years hazard levels. There are forty ground motions for each hazard level, and each ground motion consists of three components for the fault-normal, fault-parallel and vertical directions. This results in eighty ground motion records in both fault-normal and fault-parallel for each hazard level, and a total of 240 ground motion time-histories in the horizontal direction. In order to include the effect of stronger ground motions, three scaling factors are used including 1, 1.5, and 2. As a result, a total of 720 sets of ground motion records are considered for nonlinear dynamic analyses.

4. GENERATING PROBABILISTIC SEISMIC DEMAND MODEL (PSDM)

4.1. Probabilistic Seismic Demand Models

This study uses the probabilistic demand models to define a relationship between demand measures and intensity measures representing the intensity of ground motions. These models allow

estimation of the seismic performance of restrained components.

Eq. (8) is the commonly used equation for the relationship between a candidate seismic demand (D) and an intensity measure (IM), suggested by Cornell et al. (2002). Model parameters, a and b , are constants, and ε is an error term.

$$D(IM) = a \cdot IM^b \cdot \varepsilon \quad (8)$$

This equation can be changed to Eq.(9) in the logarithmic space, where a and b are transformed to \hat{a} and \hat{b} which are unbiased estimators. In this equation, the demand parameter ($\lambda_{D|IM}$) and the IM parameter ($\ln(IM)$) have a linear relationship.

$$\lambda_{D|IM} = \ln(\hat{a}) + \hat{b} \cdot \ln(IM) \quad (9)$$

However, the rocking behavior of cabinets does not fit this linear relationship (Hur and Shafieezadeh, 2013). Since the features of rocking behavior is highly nonlinear, this study used the mathematical model of loglogistic distribution for PSDMs, which is also known as the Fisk distribution. This probability distribution is continuous for a non-negative random variable whose logarithm has a logistic distribution. The cumulative distribution function can be written in closed form unlike that of the lognormal distribution as shown in Eq.(10), where α and β are model parameters.

$$F(x|\alpha, \beta) = \frac{1}{1+(x/\alpha)^{-\beta}} \quad (10)$$

Based on this equation, this study used PSDMs in the form of Eq. (11) to evaluate the relationship between the intensity measure and demand.

$$D(IM|\alpha, \beta) = \frac{1}{1+(IM/\alpha)^{-\beta}} \quad (11)$$

4.2. Engineering demands for PSDMs

PSDMs can be developed for demand measures of various components of switchboard cabinets. In general, inter-story drift, displacement, or stress are commonly adopted as important response measures for structural elements in buildings, but for the PSDMs of restrained nonstructural components such as electrical equipment,

different demand measures are needed including the deformation of restrainers, global frame drift, and relative displacement of conduits. In addition, previous studies have shown that accelerations at locations where devices are attached are also critical demands for evaluating the response of frequency-sensitive components such as electrical devices (NUREG, 1987). Among various demand measures, this study will present the ratio of the rotational displacement (θ/α) of the rigid block subjected to various seismic effects, which is an essential indicator for the tip-over failure of relatively slender electrical cabinets.

4.3. General Intensity Measures

Common intensity measures that have been used in seismic fragility analyses are peak ground acceleration (PGA) and pseudo spectral acceleration (PSA). Both of these traditional IMs have benefits and drawbacks when applied to electrical equipment. For instance, PGA may not be an appropriate IM for fragility assessment of frequency-sensitive components. Spectral acceleration (PSA_{Tn}) at a certain period is a better indicator for the performance assessment of frequency-sensitive components, but it may not be a practical measure for complex switchboard cabinets, as there can be a large number of devices affixed in a switchboard cabinet each having a different set of frequency sensitivities. That is, the fundamental frequency of the structure of electrical equipment may differ substantially from the devices attached to the structure. Therefore, the average spectral acceleration (PSA_{Avg}) is also suggested to address the disadvantages of PGA and PSA_{Tn} . (NUREG, 1987). This measure is obtained by dividing the area under a portion of the response spectrum curve (g-value vs. frequency on a regular scale) by the corresponding frequency band, which is the frequency range of interest for the particular equipment as shown in Fig. 3. Using the average spectral acceleration ensures that the response accelerations can be considered in the frequency band of interest according to IEEE Standard 344 (2005). Generally, the electrical equipment of an

indoor substation is assumed to have a frequency range of 4~16Hz unless otherwise specified.

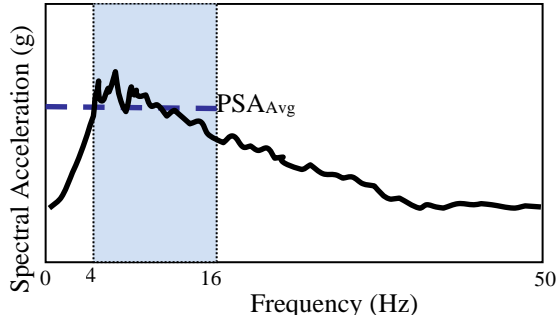


Figure 3. The Average Spectral Acceleration

Other commonly adopted IMs are peak ground velocity (PGV) and peak ground displacement (PGD) as shown in Table 6.3. This study suggests a new IM considering PGA, the total mass, and depth of sampled cabinets as shown in Eq. (12).

$$IM_{suggested} = PGA \times \frac{Mass}{Depth} = PGA \times \frac{W_{total}/g}{Depth(D)} \quad (12)$$

Table 2. Intensity Measures in this study

IMs	Definition	Units
PGA	Peak ground acceleration	g $=9.81m/sec^2$
PGV	Peak ground velocity	m/sec
PGD	Peak ground displacement	m
Suggested IM	$PGA * Mass / Depth^2$	$g * kg / m^2$ $=9.81kg / (m * sec^2)$

4.4. Effective Intensity Measures for PSDMs

The 720 sets of samples generated in section 3.1 and the scaled ground motion records explained in section 3.2 are paired and analyzed with the analytical solutions presented in section 2.2. In order to evaluate the rocking behavior, the rotational angle $\theta(t)$ of restrained blocks is computed. The nonlinear ordinary differential equations in section 2.2 are solved using the Bogachi-Shampine method (Shampine & Reichelt 1997) in MATLAB.

Figs. 4-6 show the simulation results and generated PSDMs with common intensity measures of PGA, PGV, and PGD, respectively. When the ratio of rotational angle (θ/α) reaches 1, the cabinet tips over. When the ratio is close to 0, the cabinet does not rock. Based on the simulation results, about 380 samples out of 720 do not rock nor exhibit any nonlinear behavior under various seismic shakings, while approximately 230 samples tip over under strong ground motions.

In order to evaluate the fitness of the PSDMs with different IMs to the simulation result, the coefficient of determination, R^2 , is computed as given in Eq. (13), where y is the simulated response (θ/α), and f is the predicted value.

$$R^2 = 1 - \frac{\sum_i (y_i - f_i)^2}{\sum_i (y_i - \bar{y})^2} \quad (13)$$

In Table 3, the R^2 values show that the PSDM using PGA provides an acceptable fit to the simulation results. In order to achieve a better fit, the proposed IM is applied and the results are shown in Figure 7. Even though around 85% of simulation data present the binary result (0 or 1), the loglogistic distribution model with the proposed IM provide the best fit (R^2 of 0.73) compared to commonly used IMs.

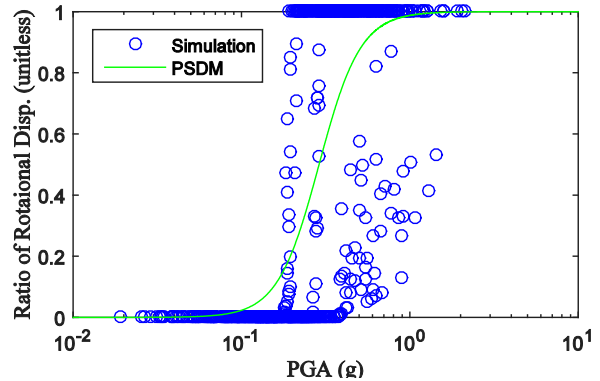


Figure 4. PSDMs using PGA

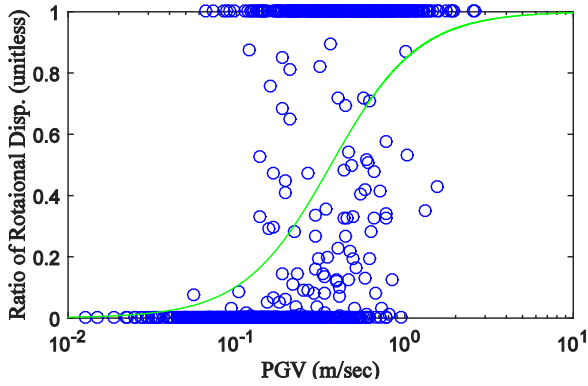


Figure 5. PSDMs using PGV

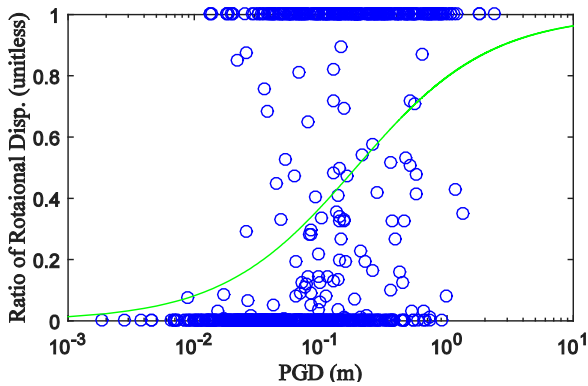


Figure 6. PSDMs using PGD

Table 3. Coefficient of Determination (R^2)

PGA	PGV	PGD	Suggested IM
0.50	0.34	0.19	0.73

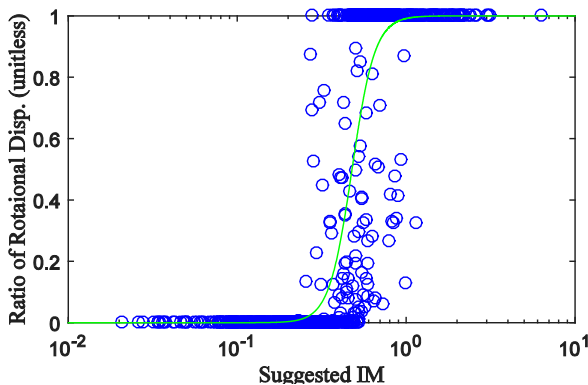


Figure 7. PSDMs using Suggested IM

5. CONCLUSIONS

This study evaluated effective intensity measures for nonlinear PSDMs of rigid electrical cabinets subjected to strong seismic shakings. In order to generate PSDMs, various parameters of electrical cabinets are considered, and 720 sets of samples are randomly generated using LHS. The resulting samples of cabinets are paired with ground motion records to conduct nonlinear time history analyses. It was observed that commonly used intensity measures such as PGA, PGV, and PGD are less effective than the new intensity measure proposed in this study for probabilistic seismic demand modeling of the cabinets. The proposed intensity measure and nonlinear loglogistic distribution model enhance the PSDMs of rigid electrical cabinets by reducing epistemic u. This PSDM will enable generation of seismic fragility functions with lower uncertainties. Results of this study provided a better understanding of the seismic performance of rigid equipment during various seismic events. This will help developing systematic and reliable decision making approaches for seismic risk management of various types of electrical cabinets.

6. REFERENCES

- Aslam et al. (1980) "Earthquake Rocking Response of Rigid Bodies", Journal of the Structural Division, 106(2): 377-392
- Baker, J. W., Lin, T., Shahi, S. K., and Jayaram, N. (2011). New Ground Motion Selection Procedures and Selected Motions for the PEER Transportation Research Program. PEER Technical Report 2011/03. 106p.
- Cornell et al. (2002) "Probabilistic basis for the 2000 SAC Federal Emergency Management Agency steel moment frame guidelines." Journal of Structural Engineering, 128(4): 526-533.
- Gupta, Abhinav, S. K. Rustogi, and Ajaya K. Gupta. "Ritz vector approach for evaluating incabinet response spectra." Nuclear engineering and design 190.3 (1999): 255-272.
- Hur (2012) "Seismic performance evaluation of switchboard cabinets using nonlinear numerical models", Georgia Institute of Technology, Georgia, Chapters 4-6
- Hur and Shafieezadeh (2013) "Characterization of Main-Shock Effects on the Aftershock Fragility of Rigid Electrical Equipment", Safety, Reliability,

Risk and Life-Cycle Performance of Structures and Infrastructures. 4415 -4421

- Makris, N. and Zhang, J. (1999), "Rocking Response and Overturning of Anchored Equipment under Seismic Excitations," PEER Report, Pacific Earthquake Engineering Research Center, College of Engineering, University of California, Berkeley
- NUREG - U.S. Nuclear Regulatory Commission (1987), "Seismic Fragility of Nuclear Power Plant Components [PHASE II]," NUREG/CR-4659, BNL-NUREG-52007, Vol. 2-4, Department of Nuclear Energy, Brookhaven National Laboratory, Long Island, NY
- Shampine, Lawrence F.; Reichelt, Mark W. (1997), "The Matlab ODE Suite", SIAM Journal on Scientific Computing 18 (1): 1-22
- Yang, Jianfeng, S. K. Rustogi, and Abhinav Gupta. "Rocking stiffness of mounting arrangements in electrical cabinets and control panels." Nuclear engineering and design 219.2 (2003): 127-141.
- Yim & Chopra (1985), "Simplified earthquake analysis of multistory structures with foundation uplift." Journal of Structural Engineering, 111(12): 2708-2731.